C$_f$/C composites: correlation between CVI process parameters and Pyrolytic Carbon microstructure

F. Burgio, P. Fabbri, G. Magnani, M. Scafè
ENEA - Faenza Technical Unit for Material Technologies (UTTMATF)
Via Ravegnana, 186 – 48018 Faenza - Italy
federica.burgio@enea.it, paride.fabbri@enea.it, giuseppe.magnani@enea.it, matteo.scafe@enea.it

L. Pilloni
ENEA, Chemical and Technology Unit (UTTMAT-CHI)
luciano.pilloni@enea.it

A. Brentari
Certimac S.c.a.r.l.
alida.brentari@enea.it

A. Brillante, T. Salzillo
University of Bologna
aldo.brillante@unibo.it, tommaso.salzillo@unibo.it

ABSTRACT. Chemical Vapour Infiltration (CVI) technique has been long used to produce carbon/carbon composites. The Pyrolytic Carbon (Py-C) matrix infiltrated by CVI could have different microstructures, i.e. Rough Laminar (RL), Smooth Laminar (SL) or Isotropic (ISO). These matrix microstructures, characterized by different properties, influence the mechanical behaviour of the obtained composites. Tailoring the process parameters, it is possible to direct the infiltration towards a specific Py-C type. However, the factors, influencing the production of a specific matrix microstructure, are numerous and interconnected, e.g. temperature, pressure, flow rates etc. Due to the complexity of the physical and chemical phenomena involved in CVI process, up to now it has not been possible to obtain a general correlation between CVI process parameters and Py–C microstructure. This study is aimed at investigating the relationship between infiltration temperature and the microstructure of obtained Py-C, for a pilot - sized CVI/CVD reactor. Fixing the other process parameters and varying only the temperature, from 1100°C to 1300°C, the Py-C infiltration was performed on fibrous preforms. Polarized light microscopy, with quantitative measurements of average extinction angle (Ae), and Raman spectroscopy were used to characterize the obtained Py-C microstructures.

KEYWORDS. C$_f$/C composites; CVI; Py-C microstructure; Temperature.

INTRODUCTION

The applications of pyrolytic carbon (Py-C) are numerous and range over many fields, such as aerospace, nuclear and medical. Pyrolytic carbon is mainly produced as matrix phase of carbon/carbon (C_f/C) composites. Thanks to their excellent mechanical properties at elevated temperatures, combined with light weight and good frictional performances, C_f/Cs are employed for the fabrication of components, as leading edges, brake discs, exit cones etc., for aerospace field. Py-C are also produced as coating material for nuclear industry, i.e. coatings of nuclear fuel particles, and in medical applications for heart valves and bone prostheses [1, 2, 3, 4]. Is widely recognized that chemical vapour infiltration (CVI) process is the ideal for obtaining high performance C_f/C composites. CVI technique allows, under mild temperature conditions, the production of pyrolytic carbon matrix with controlled composition and microstructure, without organic by-products, that required post-production treatments for their removing, and, as consequence, composites with a high degree of densification [5].

CVI process leads to Py-C with different microstructures and textures. In particular, the texture anisotropy of the Py-C matrix is a key parameter affecting the final mechanical properties of the derived C_f/Cs. Several studies have been dedicated to the Py-C classification, based on optical measurements of its anisotropy . The Py-C was classified as isotropic (ISO), dark laminar (DL), smooth laminar (SL), rough laminar (RL) and regenerative laminar (ReL) or in more general way as isotropic, low, medium and high textured [6, 7, 8]. Despite the Py-C anisotropy has been studied since the 60th, there is no clear evidence of a defined correlation between CVI process parameters and obtained Py-C structure. This probably arises from the fact that the parameters, affecting the Py-C chemical vapour infiltration, are numerous and interconnected (gaseous precursors, temperature, pressure, gas flow rates, residence time, methane/hydrogen concentration ratio, etc.) and as a consequence the literature experimental conditions are very variable [9].

The objective of this study is to point out the correlation of CVI process parameters with Py-C microstructures. As a consequence of the results gained in the previous work [10], that evidenced, at the used operating conditions, no influence of hydrogen concentration and residence time on the Py-C microstructure, here it was decided to study in particular the temperature affect. The selected process temperatures were 1100, 1200 and 1300 °C respectively, while the other process parameters, such as pressure, methane/hydrogen ratio, gas flow rates etc, were maintained constant. The Py-C chemical vapour infiltration was performed on carbon fibre preforms, by means of a pilot-sized CVI/CVD reactor. The anisotropy of the obtained Py-C was evaluated coupling the extinction angle measurements, by polarized light microscopy (PLM), with Raman analyses. The temperature effect on the Py-C infiltration behaviour was also investigated.

EXPERIMENTAL

Sample preparation

The Py-C infiltrations were performed at 3 different temperatures, 1100 °C, 1200 °C and 1300 °C, in a pilot – sized CVI/CVD plant, using methane as carbon source precursor, hydrogen as carrier gas and argon as purge gas. The other process conditions were those fixed in the previous work [10]. Tab. 1 summarizes the CVI operating conditions used for each infiltration test:

TEST	Temperature [°C]	Pressure [mbar]	Q_{CH4} [sccm]	Q_{H2} [sccm]	α	Flow rate [m/s]	τ [s]	Infiltration length [h]
CVI1	1100					0.21	3.3	100
CVI2	1200	18	800	2400	0.3	0.23	3.1	50
CVI3	1300					0.24	2.9	50

Table 1: Operating condition of the CVI experiments

where Q_i, α and τ are gas volumetric flow rate, methane/hydrogen ratio and residence time respectively.

The pilot-sized CVI/CVD plant consists of a 700 mm long cylindrical graphite reaction chamber with a 300 mm diameter, heated with graphite resistance elements. Gases are delivered into the reaction chamber, from a graphite multi-hole

distributor, in a top down direction and the continuous flow is obtained by means of two volumetric vacuum pumps. The furnace, with the gas delivery system, is shown in Fig. 1.

Figure 1: CVI/CVD plant.

Sample characterization

Polarized - light microscopy was employed to characterize the anisotropy of Py-C deposited around the carbon fibres, by the measurement of the extinction angle (A_e). The used apparatus consisted of a Zeiss microscope equipped with an halogen light source, x16 and x40 objectives, and with two rotating polarizer/analyzer. Extinction angle is the measure, expressed in deg, obtained rotating the analyzer from the Maltese cross condition to the maximum extinction of the first quadrant [11]. Fig. 2 shows the typical PLM micrographs, where are evident the Maltese crosses of the Py-C matrix around the carbon fibres. In particular these micrographs are related to the C_f/C composites obtained at 1300 °C.
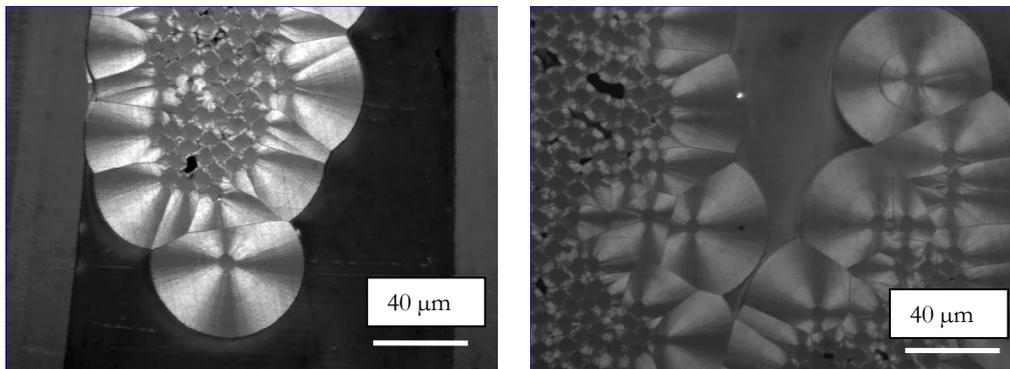

Figure 2: PLM micrographs of Py-C deposited around the carbon fibres at 1300 °C.

The extinction angle is related to the Py-C anisotropy and has been long used to classify the large number of Py-C [11, 12]. Tab. 2 summarizes the typical values of A_e and the density of the different Py–C optical textures [11, 13, 14].

Optical texture	Domain of extinction angle A_e	Density
Rough Laminar (RL)	≥ 18°	2.0 – 2.2
Smooth Laminar (SL)	12° - 18°	1.8 – 1.9
Dark Laminar (DL)	4° - 12°	1.6 – 1.8
Isotropic (ISO)	< 4°	< 1.6

Table 2: classification of Py-C optical texture.

The degree of crystallinity and the micro-structural features of the Py-C, obtained at the different temperatures, were also investigated by Raman analyses. Raman spectra were collected using a Renishaw single grating spectrometer, equipped with a suitable notch filter and CCD detector. The Raman scattering was excited using an Ar^+ laser tuned at 514.5 nm with 25 mW of power. The spectrometer was interfaced to an optical microscope (Olympus BX40) with x50 or x100 objectives, which produced a spatial resolution from about 0.75 to 1 µm, with a theoretical field depth ranging from about 7 to 25 µm. The incoming laser output power was reduced with a neutral filter, whose optical density was selected in each experiment to prevent sample damage, the actual power focused on the sample being anyway always less than 1 mW.

The bulk density of the produced C_f/Cs was derived from their volume measurements, with an helium pycnometer (AccuPyc 1330 Pycnometer – Micromeritics).

Furthermore, in order to study the infiltration behaviour, the steady-state deposition rates ($R_{deposition}$) of Py-C were determined by SEM (SEM Leo 438 VP equipped with EDS – Link ISIS 300) measurements of the Py-C thickness, deposited on the inner and outer fibres of the C_f/C composites. The infiltration behaviour was also analyzed by optical microscopy observations (Reichert – Jung MeF3) of the C_f/Cs. All the optical analyses were performed on C_f/C polished cross sections.

RESULTS

The measured extinction angle values were in the range of 4 to 8 degrees, for all the temperature conditions: this could be an indication of a dark laminar texture [11, 13, 14]. Despite the easiness and rapidity of the A_e measurement method, it can be employed only as a qualitative indication of the Py-C texture. This is mainly due to the fact that the measurements are affected by human eye sensitivity, not able to individuate the minimum intensity conditions with high accuracy [12].

More detailed information, regarding the influence of temperature on Py-C microstructures, was derived from Raman analyses. The recorded spectra were those typical of Py-C, with two first-order bands, the disorder - induced D and the graphite - induced G at 1360 and 1580 cm^{-1} respectively, and two second-order bands at 2700 and 2900 cm^{-1}. Fig. 3 summarizes the obtained spectra. The comparison of the obtained Raman spectra with literature ones, did not evidence a clear correspondence with SL, RL or ReL Py-C spectra [15]. This could support the hypothesis of a DL texture. Dark laminar is a Py-C transition structure between isotropic and smooth laminar ones: it has low density and weak anisotropy [16]. As a consequence, it is not being considered of technological interest, the related Raman spectra are not available in literature.
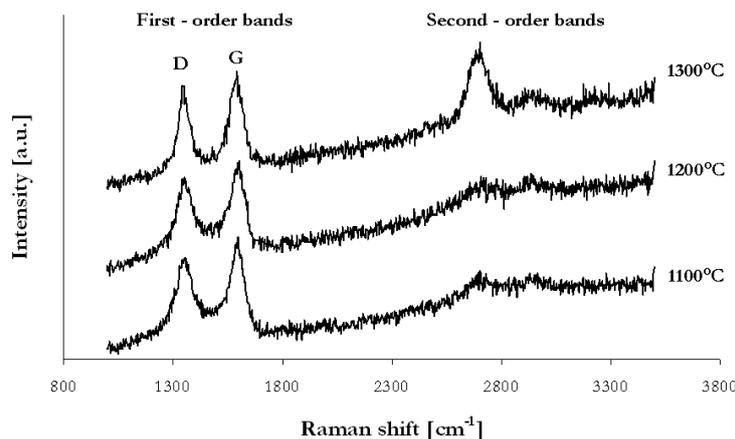

Figure 3: Raman spectra of Py-C deposited at 1100, 1200 and 1300 °C.

However, the Raman analyses evidenced differences in the order and crystallinity of the Py–C obtained at increasing temperatures. In particular, it was evidenced that the Py-C structures exhibited an increasing degree of structural ordering and graphitization with the temperature increasing. It could be deduced from many parameters. Firstly from the intensity ratio of D and G bands (I_D/I_G), that is inversely proportional to the degree of graphitization [2, 17]. Fig. 4 shows that the higher the temperature, the lower the I_D/I_G ratio. Secondly, it was deduced from the decreasing of the full width at half maximum (FWHM) intensity of the D bands with the temperature, as shown in Fig. 5. The full width at half maximum

(FWHM) of the D band has been correlated to the in-plane structural ordering, in particular the larger the $FWHM_D$, the higher the structural disorder [15, 18].

Furthermore, with the temperature increasing the second-order band became more evident (Fig. 3). The second-order band has been related to the three dimensional order. So, it could be deduced that at 1300°C a more ordered structured Py-C was obtained.
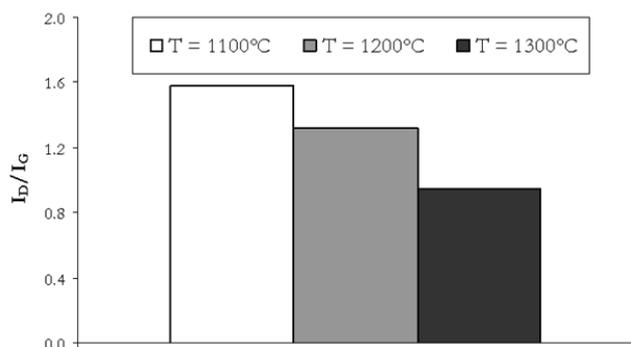

Figure 4: Intensity ratio of D and G bands of Py-C deposited at 1100, 1200 and 1300 °C.
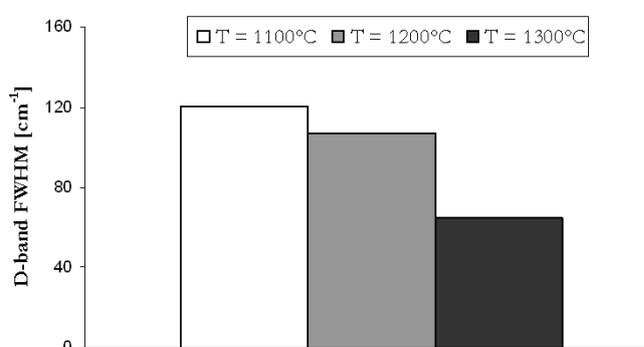
Figure 5: Full width at half maximum (FWHM) of the D band of Py-C deposited at 1100, 1200 and 1300 °C.

After the Py-C matrix infiltration, there was a bulk density decrease from the starting value of the fibre preforms, 1.8 g/cm³, to the final average value of the composites, 1.6 g/cm³, at all the infiltration temperatures. The values are reported in Fig. 6 as a function of the CVI temperature and the sample distance from the gas inlet in the reaction chamber.

The C_f/C density decrease could be reasonably ascribed to the low density of the Py-C infiltrated. This hypothesis was also confirmed by SEM observations of the Py–C microstructures. In Fig. 7, SEM micrograph highlights the high degree of porosity of the Py –C. The low density and the high porosity of the Py-C supported the initial hypothesis of a dark laminar texture obtained at all the operating temperatures here investigated.
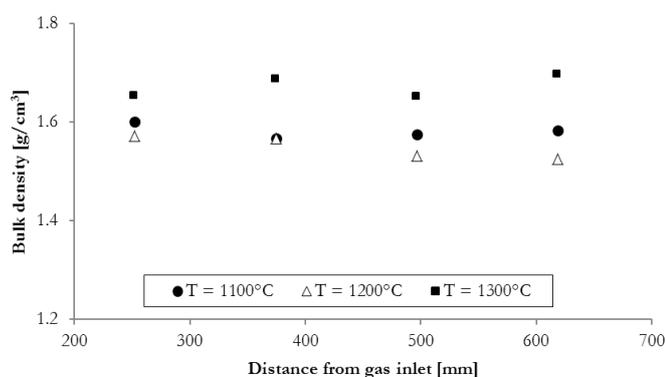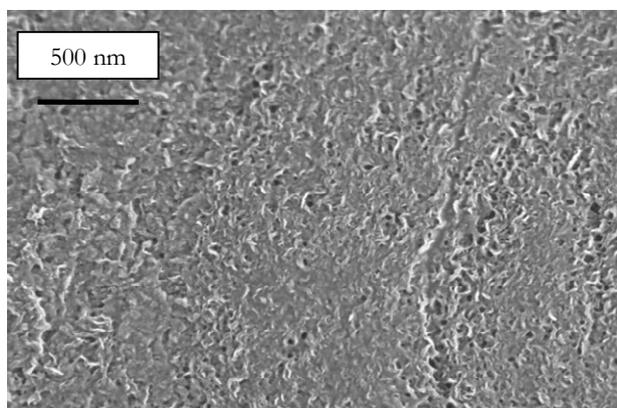

Figure 6: C_f/C bulk density.

Figure 7: SEM micrographs of Py-C.

The Py–C steady – state deposition rates are summarized in Tab. 3, in correlation with the temperature and the residence time of the infiltration processes. It was evident that only at 1200 °C the inner and the outer deposition rate values were comparable, while at 1100 °C and 1300 °C the two values were widely different and in both cases the inner deposition rate resulted lower than the outer one. The differences between the Py–C inner and outer values of deposition rate, for the 3 temperatures, resulted in a different infiltration behaviour of the C_f/Cs as is shown in Fig. 8. The optical images of the C_f/C cross sections, for each process temperature, evidences the effect of deposition rate on the preform infiltration mode. At 1100 and 1300 °C, the Py-C was mainly deposited on the outer fibres, instead at 1200 °C its intermediate value of deposition rate allowed a more uniform Py-C infiltration between inner and outer fibres.

The resulting different infiltration behaviour was probably due to the different residence time of the process gases, as already evidenced in the previous work [10]. At low residence times, and therefore at high flow rates, methane has no sufficient time to diffuse inside the inner porosities: this is the condition occurred at 1300 °C. On the other side, at higher

residence times and lower flow rates, 1100 °C situation, the hydrogen, flowed in the internal porosities, has sufficient time to inhibit the methane decomposition lowering the deposition rate. At 1200°C, with intermediate values of both residence time and flow rate, a compromise condition between diffusion and inhibition was established.

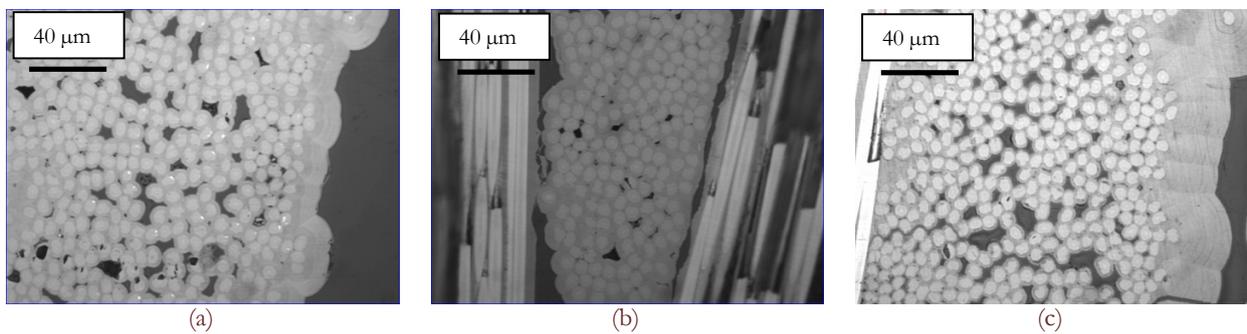| Temperature	Residence time	Flow rate	Deposition rate [μm/h]	
[°C]	[s]	[m/s]	From Py-C thickness of the inner fibres	From Py-C thickness of the outer fibres
1100	3.3	0.21	0.06	0.12
1200	3.1	0.23	0.11	0.13
1300	2.9	0.24	0.02	0.7

Table 3: steady – state Py-C deposition rates.

Figure 8: Optical micrographs the C_f/C cross sections at (a) 1100 °C, (b) 1200 °C and (c) 1300 °C.

CONCLUSIONS

The effects of CVI temperature on Py-C microstructure and infiltration behaviour have been investigated. It was found that the temperature variation in the range of 1100 to 1300 °C, at the operating condition here considered, did not affect the Py-C texture: a dark laminar Py-C was indeed obtained at all the analyzed conditions of temperature. The dark laminar texture was identified by extinction angle measurements. Raman analyses evidenced the temperature influence on microstructural order and on degree of graphitization of the obtained pyrolytic carbon: at the higher temperature (1300 °C) a more ordered and graphitized Py-C microstructure was obtained. Moreover, the process temperature affected the infiltration behaviour: at 1200 °C the Py-C infiltration resulted more homogeneous than at the other two temperatures, in terms of internal and external porosities densification.

In order to obtain a dense C_f/C with high mechanical properties two main features are required: an optimum value of residence time, that allows a gradual reduction of the porosities, and a Py-C matrix microstructure with high density. The results, obtained in this work, allowed to fix the residence time obtained at 1200 °C, 3.1 s, as an optimal value from the point of view of the infiltration behaviour. The change of the alfa values could lead to the obtaining of Py-C structure with higher density.

REFERENCES

[1] Lopez-Honorato, E., Meadows P.J., Xiao P., Fluidized bed chemical vapor deposition of pyrolytic carbon – I. Effect of deposition conditions on microstructure, Carbon, 47 (2009) 396-410.

[2] Zou, L., Huang, B., Huang, Y., Huang, Q., Wang, C., An investigation of heterogeneity of the degree of graphitization in carbon–carbon composites, Materials Chemistry and Physics, 82 (2003) 654–662.

[3] Ozcan, S., Filip, P., Microstructure and wear mechanisms in C/C composites, Wear, 259 (2005) 642–650.

[4] Chen, T., Gong, W., Liub, G., Zhang, F., Influence of graphite foils on I-CVI densification rate and microstructure of obtained pyrolytic carbon of carbon–carbon composites, Composites: Part A, 36 (2005) 1494–1498.

[5] Naslain R., Design, preparation and properties of non-oxide CMCs for application in engines and nuclear reactors: an overview, Composites Science and Technology, 64 (2004) 155-170.

[6] Reznik, B., Huttinger, K.J., On the terminology for pyrolytic carbon, Carbon, 40 (2002) 617 –636.

[7] Bortchagovsky, E.G., Reznik, B., Gerthsen, D., Pfrang, A., Schimmel, Th., Optical properties of pyrolytic carbon deposits deduced from measurements of the extinction angle by polarized light microscopy, Carbon, 41 (2003) 2427 – 2451.

[8] Bourrat, X., Langlais, F., Chollon, G., Vignoles, G., Low Temperature Pyrocarbons: A Review, J. Braz. Chem. Soc., 17, (2006) 1090-1095.

[9] Oberlin, A., Review Pyrocarbons, Carbon, 40 (2002) 7–24.

[10] Burgio, F., Pilloni, L., Labanti, M., Scafè, M., Brentari, A., Falconieri, M., Sangiorgi, S., Validation of Py-C chemical vapour deposition and infiltration process codes, In: Proceeding of 15th European Conference on Composite Materials and Oral Presentation, Venice, Italy (2012).

[11] Bourrat, X., Trouvat, B., Limousin, G., Vignoles, G., Pyrocarbon anisotropy as measured by electron diffraction and polarized light, J. Mater. Res., 15 (2000).

[12] Vallerot, J.M., Bourrat, X., Pyrocarbon optical properties in reflected light, Carbon, 44 (2006) 1565–1571.

[13] Dupel, P., Bourbat, X., Pailler, R., Structure of pyrocarbon infiltrated by pulse-CVI, Carbon, 33 (1995) 1193-1204.

[14] Morgan, P., Carbon fibers and their composites, Taylor & Francis Group, (2005).

[15] Vallerot, J.M., Bourrat, X., Mouchon, A., Chollon, G., Quantitative structural and textural assessment of laminar pyrocarbons through Raman spectroscopy, electron diffraction and few other techniques, Carbon 44 (2006) 1833–1844.

[16] Bourrat, X., Structure of pyrocarbons, in Delhaès P. (Eds.), Fibers and composites, Taylor & Francis, 8 (2003).

[17] Zhang, D., Li, K., Li, H., Guo L., Lu, J., The influence of deposition temperature on the microstructure of isotropic pyrocarbon obtained by hot-wall chemical vapor deposition, J Mater Sci, 46 (2011) 3632–3638.

[18] Bourrat, X., Pyrocarbon performances and characterization, In: Proceed. Carbon'09, World Conf on Carbon, Biarritz (2009) T11-ID 792.